ELSEVIER

Polymer 40 (1999) 6761–6768

polymer

Phase behaviors of hyperbranched polymer solutions

Jeong Gyu Jang, Young Chan Bae*

Department of Industrial Chemistry and Molecular Thermodynamics Laboratory, Hanyang University, Seoul 133-791, South Korea

Received 17 August 1998; received in revised form 19 October 1998; accepted 21 December 1998

Abstract

We developed a new model based on the lattice cluster theory to describe phase behaviors of binary hyperbranched polymer solution systems. To account for highly oriented interactions between segments, the proposed model requires an additional parameter ($\delta\varepsilon/k$) related to the energy of the oriented interaction. A thermo-optical analysis (TOA) technique was used to determine cloud-points for the given systems. Hyperbranched polyol/water systems exhibit an upper critical solution temperature (UCST) behavior.

Keywords: Hyperbranched polymer; Dendritic polymer; Lattice cluster theory

1. Introduction

In recent years, dendritic polymers (dendrimer and hyperbranched polymers) have enjoyed increased attention. The backbone architecture induces new and intriguing properties for the polymers, such as low viscosity, miscibility, high reactivity and high solubility in various solvents [1].

Many potential applications for dendritic polymers have been proposed [2]. Most of the ideas focus on the peculiarities of the dendritic interior and a large number of endgroups for their rationalization. The behavior of dendritic polymers as hosts is essential if they are to be successfully used as solubilizing agents, nanoscale catalysts [3] and drug delivery and slow release agents for perfumes, herbicides and drugs. Research is also active in applications as diverse as polymer additives, catalyst supports, thin films, laser-printing toners and magnetic resonance imaging (MRI) contrast agents. Despite the wealth of possible applications, there are only a few studies on the thermodynamic properties of solutions containing dendritic polymers.

The standard lattice model of polymers was solved in the simple mean field approximation independently by Flory [4] and Huggins [5] and the treatment of the former is customarily termed Flory–Huggins theory. In addition, much work has been performed on improving the mathematical solution of the lattice model including chain connectivity and non-random mixing [6]. However, the mean field approximation has been found to be quantitatively deficient in some aspects. To consider the entropic contribution of the interaction parameter, χ, which is of purely enthalpic origin in the model, Koningsveld and Kleintjens [7] derived a closed form expansion for the interaction parameter considering the nearest neighbor site occupancy probability. In a lattice dependent fashion that, however, it is difficult to interpret in comparison with the experimental data.

Taking into account the compressibility and change in density upon isothermal mixing, free volume theories for polymer solutions were developed by numerous investigations, notably by Flory [8,9], Patterson and Delmas [10], and Sanchez and Lacombe [11].

The lattice models are supplemented by an entropic contribution to interaction energies. Barker and Fock [12] developed a quasi-chemical method to account for the specific interaction. ten Brinke and Karasz [13] have developed an incompressible model of binary mixture with the specific interaction. Using a quasi-chemical approach to treat the non-random character of the polymer solution, Panayiotou and Vera [23] and Renucio and Prausnitz [24] have developed an improved FOVE equation of state model and Panayiotou [25], and Sanchez and Balazs [26] have generalized the lattice fluid model to account for the specific interaction of the compressible model.

Further, Freed et al. [14–16] reported a complicated lattice field theory for polymer solutions, which is formally an exact mathematical solution of the Flory–Huggins lattice. However, most of these lattice theories fail to yield a dependence of solution properties on the polymer architecture. Recently, Freed et al. [17–22] developed a systematic expansion of the partition function of a lattice

* Corresponding author. Tel.: + 82-2-290-0529; fax: + 82-2-296-6280.
E-mail address: ycbae@email.hanyang.ac.kr (Y.C. Bae)

0032-3861/99/$ - see front matter
PII: S0032-3861(99)00005-1

Table 1
Geometric parameters for linear and dendritic polymers

	Linear	Dendrimer
M	$n + 1$	$3(2^{g-1} - 1)n + 1$
N_1	n	$3(2^{g-1} - 1)n$
N_2	$n - 1$	$3(2^{g-1} - 1)(n - 1) + 3N_\perp$
N_3	$n - 2$	$3(2^{g-1} - 1)(n - 2) + 6N_\perp$
$N_\perp$	0	$3(2^{g-2} - 1) + 1$
$N_{1,1}$	$(n - 1)(n - 2)/2$	$3(2^{g-1} - 1)(n - 1)(n - 2)/2 + 3(2^{g-1} - 1)[3(2^{g-1} - 1) - 1]n^2/2 - 3N_\perp$
$N_{1,2}$	$(n - 2)(n - 3)$	$3(2^{g-1} - 1)(n - 2)(n - 3) + 3N_\perp(N_1 - 5) + 3(2^{g-1} - 1)[3(2^{g-1} - 1) - 1]n(n - 1) - 6N_\perp$

polymer using the well-known lattice cluster theory (LCT). This model takes into account the effect of branching on the thermodynamic properties of polymer solutions. Lue and Prausnitz [28] applied the LCT to obtain solvent activities and liquid–liquid equilibria for homogeneous-dendrimer polymers.

In this study, we investigated liquid–liquid equilibria of hyperbranched polymer solutions (Tables 1 and 2). The experimental technique used to determine the cloud points of the systems was the thermo-optical analysis (TOA) technique. To predict phase behaviors of the systems, we modified the LCT model to account for strongly interacting components by employing the concept of the generalized lattice fluid (LF) model [13,26].

2. Experimental

2.1. Materials

The hyperbranched polyols, generation 2, 3 and 4 were purchased from Aldrich Chemical Co. (44706-4, 44707-2, 44708-0). All polymer samples were used with no further purification. Distilled deionized water was used as a solvent.

The weight average molecular weight (M_w) and polydispersity indices are listed in Table 3.

2.2. Sample preparation

Samples were prepared in separate test tubes and the composition of each sample was precisely measured gravimetrically. Each solution was stirred for 5 h or more. The solution was then transferred to a Pyrex tube (i.d. = 1 mm, o.d. = 3 mm, length = 50 mm) and the sample tube was flame-sealed under nitrogen atmosphere. The cloud-point curves were determined at the saturated vapor pressure of the solvent.

Table 2
The structures of the polymers[a]

Hyperbranched polyol	Structure
Gen. 2	$[O[CH_2C(CH_2H_5)(CH_2O-)_2]_2A_4B_8$
Gen. 3	$[O[CH_2C(CH_2H_5)(CH_2O-)_2]_2A_4A_8B_{16}$
Gen. 4	$[O[CH_2C(CH_2H_5)(CH_2O-)_2]_2A_4A_8A_{16}B_{32}$

[a] A = [COC(CH3)(CH2O–)2]; B = [COC(CH3)(CH2OH)2].

2.3. Thermo-optical analysis apparatus

Thermo-optical analysis (TOA) apparatus consists of a heating–cooling stage, a photodiode (Mettler FP82) and a microprocessor (Mettler FP90). An IBM PC was used as a data acquisition system.

The heating stage is designed for observation of the thermal behavior of a sample under the microscope. Luminosity in the observation field is measured by a photodiode and recorded on the PC. In this stage, the sample temperature is controlled by both upper and lower plates, assuming symmetric heat distribution throughout the sample. In this way, equilibrium time can be shortened as the sample cell is only ∽0.02 ml. Cloud points of the given systems were determined with a scan rate of 2.0°C/min.

3. Theoretical consideration

3.1. Lattice cluster theory

Freed et al. [14,15] proposed a lattice cluster theory (LCT) for homogeneous dendrimers. In this model, they used a classical lattice scheme as follows: a polymer solution occupies a lattice with the total number of lattice N_l, each monomer or a solvent molecule occupy one lattice and each polymer molecule is assumed to occupy M lattice sites. The lattice is incompressible, that is, the lattice is assumed to be fully occupied.

Volume fractions of polymer (ϕ_2) and solvent (ϕ_1) in solution are

$$\phi_1 = N_s/N_l, \tag{1}$$

$$\phi_2 = N_p M/N_l, \tag{2}$$

where N_p and N_s are the number of polymer molecules and the number of solvent molecules in solution, respectively.

Lattice sites have z nearest neighbors, giving z possible directions for the bonds emanating from a given lattice. ε_{ps} is the attractive interaction energy. The free energy is given in a double expansion series with $1/z$ and $\beta\varepsilon_{ps}(\beta = 1/kT)$. We truncate the series at the fourth order in $1/z$ and the

Table 3
Experimental cloud-point data for hyperbranched polyol in water

Gen. 2 ($M_w = 1.750$, $M_w/M_n = 1.44$)		Gen. 3 ($M_w = 3.600$, $M_w/M_n = 1.30$)		Gen. 4 ($M_w = 7.300$, $M_w/M_n = 1.18$)	
ϕ_p	T(K)	ϕ_p	T(K)	ϕ_p	T(K)
0.050	321.6	0.020	380.1	0.020	406.3
0.050	322.4	0.020	386.5	0.050	436.3
0.053	324.6	0.100	396.7	0.100	430.1
0.060	327.9	0.150	395.4	0.150	425.3
0.088	329.4	0.191	394.2	0.200	421.9
0.100	330.2	0.250	378.5	0.250	413.5
0.151	333.0	0.302	366.5	0.298	312.4
0.229	336.2	0.399	330.1	0.349	331.7
0.249	338.1	0.413	331.3		
0.276	341.6	0.344	334.4		
0.290	341.4				
0.299	341.5				
0.327	341.6				
0.375	341.0				
338.4					

second order in $\beta\varepsilon_{ps}$. The free energy of mixing for the polymer–solvent system is given by [27].

$$\Delta A = \Delta A^{ath} + \Delta A^{int} \tag{3}$$

where ΔA^{int} and ΔA^{ath} are the contribution of the attractive interaction and the athermal limit of the entropy of mixing, respectively.

$$\begin{aligned}\frac{\beta\Delta A^{int}}{N_l} &= A^{(1)}\phi_2(1-\phi_2) + (A^{(2)} + B^{(3)})\phi_2^2(1-\phi_2)^2 \\ &+ A^{(3)}\phi_2^2(1-\phi_2)^2(1-2\phi_2)^2 + A^{(4)}\phi_2^2(1-\phi_2)^2 \\ &\times[1 - 6\phi_2(1-\phi_2)(3\phi_2^2 - 3\phi_2 + 2)] + (B^{(1)} \\ &+ B^{(2)})\phi_2(1-\phi_2)^2 + B^{(4)}\phi_2^3(1-\phi_2)^2 \\ &+ C^{(1)}\phi_2(1-\phi_2)^2(1-2\phi_2)^2 + C^{(2)}\phi_2(1-\phi_2)^3 \\ &+ C^{(3)}\phi_2^2(1-\phi_2)^3(1-3\phi_2) + C^{(4)}\phi_2(1-\phi_2)^4,\end{aligned} \tag{4}$$

where

$$A^{(1)} = \frac{\beta\varepsilon z}{2}, \tag{5}$$

$$A^{(2)} = -\frac{(\beta\varepsilon)^2 z}{4}, \tag{6}$$

$$A^{(3)} = -\frac{(\beta\varepsilon)^3 z}{12}, \tag{7}$$

$$A^{(4)} = -\frac{(\beta\varepsilon)^4 z}{48}, \tag{8}$$

$$B^{(1)} = -\beta\varepsilon N(1), \tag{9}$$

$$B^{(2)} = \frac{\beta\varepsilon}{z}(2N(2) + N(3) + 3N(\perp) + N(1,2) - N(1)N(2)M), \tag{10}$$

$$B^{(3)} = -\frac{2\beta\varepsilon}{z}N(1)(2N(1) + N(1,1) - [N(1)]^2 M), \tag{11}$$

$$B^{(4)} = -\frac{4\beta\varepsilon}{z}[N(1)]^3, \tag{12}$$

$$C^{(1)} = -\frac{(\beta\varepsilon)^2}{z}N(1), \tag{13}$$

$$C^{(2)} = -(\beta\varepsilon)^2 N(2), \tag{14}$$

$$C^{(3)} = -(\beta\varepsilon)^2[N(1)]^2, \tag{15}$$

$$C^{(4)} = -\frac{(\beta\varepsilon)^2}{2}(N(1,1) - [N(1)]^2 M), \tag{16}$$

$$\begin{aligned}\frac{\beta\Delta A^{ath}}{N_l} &= \frac{\phi_2}{M}\ln\phi_2 + (1-\phi_2)\ln(1-\phi_2) \\ &+ a^{(0)}\phi_2(1-\phi_2) + a^{(1)}\phi_2^2(1-\phi_2) \\ &+ a^{(2)}\phi_2^3(1-\phi_2),\end{aligned} \tag{17}$$

where

$$a^{(0)} = \frac{1}{z}[N(1)]^2 + \frac{1}{z^2}\{ -4N(1)N(2) + \frac{8}{3}[N(1)]^3 - 2N(1)N(3) + [N(2)]^2 - 2N(1)(N(1,2) - N(1)N(2)M) + 2[N(1)]^4 + 2[N(1)]^2 \times (N(1,1) - [N(1)]^2M) - 6N(1)N(\perp)\}, \quad (18)$$

$$a^{(1)} = \frac{1}{z^2}\left[\frac{8}{3}[N(1)]^3 + 2[N(1)]^4 + 2[N(1)]^2(N(1,1) - [N(1)]^2M)\right], \quad (19)$$

$$a^{(2)} = \frac{1}{z^2}2[N(1)]^4, \quad (20)$$

where $N(\alpha) = N_\alpha/M$ ($\alpha = 1,2,3$ or $\perp$) and $N(\alpha\beta) = N_{\alpha,\beta}/M$ ($\alpha = 1$ or 2).

The combinatorial numbers, N_α and $N_{\alpha\beta}$, describe the architecture of polymers. The definitions [17–20] of the structure parameters are given as follows: M is the number of segments in each polymer molecule. N_1 is the number of bonds in each polymer molecule. N_2 is the number of ways in which three bonds intersect. N_3 is the number of ways in which three consecutive bonds can be chosen. $N_\perp$ is the number of ways in which three bonds meet at a lattice site for a polymer chain. $N_{1,1}$ is the number of distinct ways of selecting two non-sequential bonds on the same chain. $N_{1,2}$ is the number of distinct ways of selecting one bond and two sequential bonds on the same chain.

In the LCT model, the linear polymers are characterized by a single parameter, n, the total number of bonds, $M = n + 1$, and the dendritic polymers consist of a central core with three arms; the dendrimer structure is characterized by two parameters, the generation number (g) and the separator length (n) that is the number of bonds between branch points. The combinatorial numbers, N_α and $N_{\alpha\beta}$, are calculated by counting indices for these types of polymers. Geometric parameters for linear and dendritic polymers are listed in Table 1.

3.2. Interaction energy

In the LCT, van der Waals attractive energies (ε_{22}, ε_{11} and ε_{12}) are present between nearest-neighbor monomers, solvent molecules, and polymer–solvent pairs. The attractive interaction in the system is characterized by parameter ε,

$$\varepsilon = \varepsilon_{22} + \varepsilon_{11} - 2\varepsilon_{12}. \quad (21)$$

Sanchez and Balazs [19] have developed the generalized lattice fluid model to account for strongly interacting components. The basic idea is that for two components to interact strongly, they must be in proper orientation with respect to one another; i.e. there is a specific spatial or geometric constraint on the interaction (specific interaction). Other mutual orientations of the interacting pairs are energetically less favorable, but many more of them may exist. Thus, an entropic contribution must be paid to form a specific interaction. Sanchez et al. [26] have adopted a similar approach to that of ten Brinke and Karasz [13], who have developed an incompressible model for a binary mixture with specific interaction. To account for the entropic contribution by the specific interaction between a monomer–solvent pair, we employ this approach to the LCT. A detailed description of this procedure is reported elsewhere [26].

The polymer–solvent interaction can be weak (non-specific) with energy ε_{12} or strong (specific) with energy $\varepsilon_{12} + \delta\varepsilon$. The new energy parameter f_{12}, which accounts for the specific interaction, is given by

$$f_{12} = \varepsilon_{12} + \delta\varepsilon - \mathrm{kT}\ln\left[\frac{1+q}{1+q\exp(-\beta\delta\varepsilon)}\right], \quad (22)$$

where $\beta = 1/\mathrm{kT}$, q is the number of ways that the non-specific 1-2 interaction occurs. In this approach, the purely energetic parameter has been replaced by the free energy parameter f_{12}. Thus, Eq. (22) is rewritten as follows:

$$\varepsilon_{ps} = \varepsilon_{11} + \varepsilon_{22} - 2f_{12} = \varepsilon - 2\delta\varepsilon + 2\mathrm{kT}\ln\left[\frac{1+q}{1+q\exp(-\beta\delta\varepsilon)}\right], \quad (23)$$

where $\varepsilon = \varepsilon_{22} + \varepsilon_{11} - 2\varepsilon_{12}$.

The chemical potential of the solvent, $\Delta\mu_1$, can be determined from the Helmholtz free energy,

$$\Delta\mu_1 = \frac{\Delta A}{N_l} - \phi_2\frac{\partial\Delta A/N_l}{\partial\phi_2}, \quad (24)$$

$$\beta\Delta\mu_1 = \ln(1-\phi_2) + \left(1 - \frac{1}{M}\right)\phi_2 + a^{(0)}\phi_2^2 - a^{(1)}\phi_2^2 \times (1-2\phi_2) - a^{(2)}\phi_2^3(2-3\phi_2) + A^{(1)}\phi_2^2 - (A^{(2)} + B^{(3)})\phi_2^2(1-\phi_2)(1-3\phi_2) - A^{(3)}\phi_2^2(1-\phi_2)(1-2\phi_2)(1-9\phi_2+10\phi_2^2) - A(4)\phi_2^2(1-\phi_2)(1-27\phi_2+138\phi_2^2-294\phi_2^3 + 306\phi_2^4 - 126\phi_2^5) + (B^{(1)} + B^{(2)})2\phi_2^2(1-\phi_2) - B^{(4)}2\phi_2^3(1-\phi_2)(1-2\phi_2) + C^{(1)}2\phi_2^2(1-\phi_2) \times (1-2\phi_2)(3-4\phi_2) + C^{(2)}3\phi_2^2(1-\phi_2)^2 - C^{(3)}\phi_2^2(1-\phi_2)^2(1-10\phi_2+15\phi_2^2) + C^{(4)}4\phi_2^2(1-\phi_2)^3. \quad (25)$$

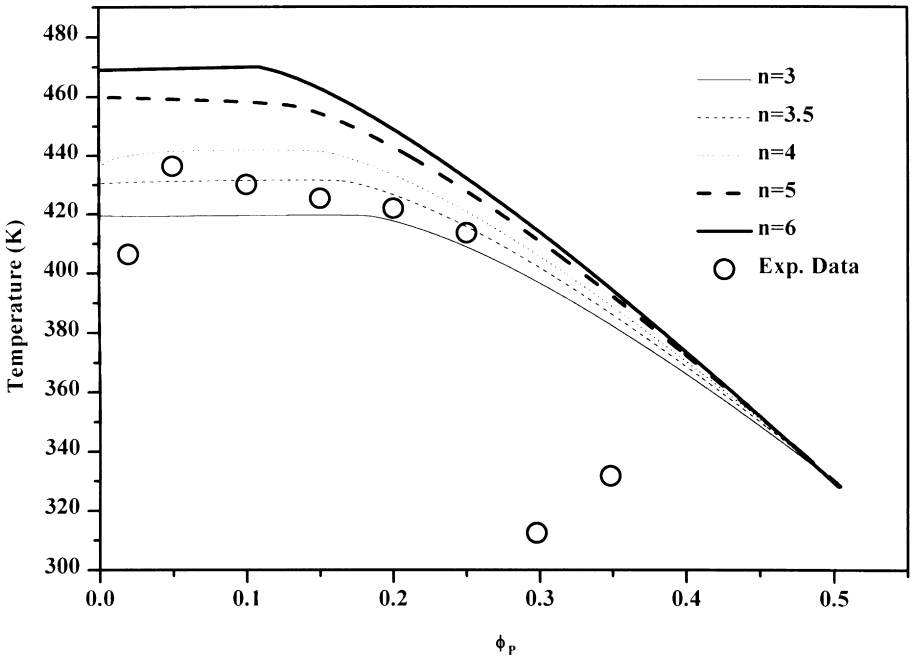

Fig. 1. Coexistence curves for the hyperbranched polyol gen. 4($M_w = 7.300$)/water system. Coexistence curves are calculated from the LCT with the separator length (n). ○ indicate experimental data.

Similarly, the chemical potential of the polymer, $\Delta\mu_2$, is

$$\Delta\mu_2 = \frac{\Delta A}{N_l} + (1-\phi_2)\frac{\partial \Delta A/N_l}{\partial \phi_2}, \tag{26}$$

$$\begin{aligned}\beta\Delta\mu_2 = {} & \frac{\ln\phi_2}{M} - \left(1-\frac{1}{M}\right)(1-\phi_2) + a^{(0)}(1-\phi_2)^2 \\ & - a^{(1)}2\phi_2(1-\phi_2)^2 + a^{(2)}3\phi_2^2(1-\phi_2)^2 \\ & + A^{(1)}(1-\phi_2)^2 + (A^{(2)}+B^{(3)})\phi_2(1-\phi_2)^2 \\ & \times(2-3\phi_2) + A^{(3)}\phi_2(1-\phi_2)^2(1-2\phi_2) \\ & \times(2-11\phi_2+10\phi_2^2) + A(4)\phi_2(1-\phi_2)^2 \\ & \times(2-39\phi_2+168\phi_2^2-330\phi_2^3+324\phi_2^4-126\phi_2^5) \\ & + (B^{(1)}+B^{(2)})(1-2\phi_2)(1-\phi_2)^2 \\ & + B^{(4)}\phi_2^2(1-\phi_2)^2(3-4\phi_2) \\ & + C^{(1)}(1-\phi_2)^2(1-2\phi_2) \\ & \times(1-8\phi_2+8\phi_2^2) + C^{(2)}(1-\phi_2)^3(1-3\phi_2) \\ & + C^{(3)}\phi_2(1-\phi_2)^3(1-5\phi_2)(2-3\phi_2) \\ & + C^{(4)}(1-\phi_2)^4(1-4\phi_2). \end{aligned} \tag{27}$$

For the critical point,

$$\frac{\partial\Delta\mu_2}{\partial\phi_2} = 0, \qquad \frac{\partial^2\Delta\mu_2}{\partial\phi_2^2} = 0, \tag{28}$$

where

$$\begin{aligned}\frac{\partial\beta\Delta\mu_2}{\partial\phi_2} = {} & 1 - \frac{1}{M}\left(1-\frac{1}{\phi_2}\right) - 2a^{(0)}(1-\phi_2) \\ & + a^{(1)}(3\phi_2^2-4\phi_2+1) \\ & + 3a^{(2)}(4\phi_2^3-6\phi_2^2+2\phi_2) \\ & + A^{(1)}(\phi_2-1) + (A^{(2)}+B^{(3)})(2-14\phi_2 \\ & + 24\phi_2^2-12\phi_2^3) + A^{(3)}(2-38\phi_2+192\phi_2^2 \\ & - 396\phi_2^3+360\phi_2^4-120\phi_2^5) + (B^{(1)}+B^{(2)}) \\ & \times 2(1-\phi_2)(3\phi_2-2) + B^{(4)}2(\phi_2-1) \\ & \times\phi_2(-3+12\phi_2-10\phi_2^2) + C^{(1)}2(1-\phi_2) \\ & \times(-6+39\phi_2-72\phi_2^2+40\phi_2^3) + C^{(2)}6 \\ & \times(\phi_2-1)^2(2\phi_2-1) + C^{(3)}2(\phi_2-1)^2 \\ & \times(1-17\phi_2+55\phi_2^2-45\phi_2^3) + C^{(4)}4(2-5\phi_2) \\ & \times(-1+\phi_2)^3, \end{aligned} \tag{29}$$

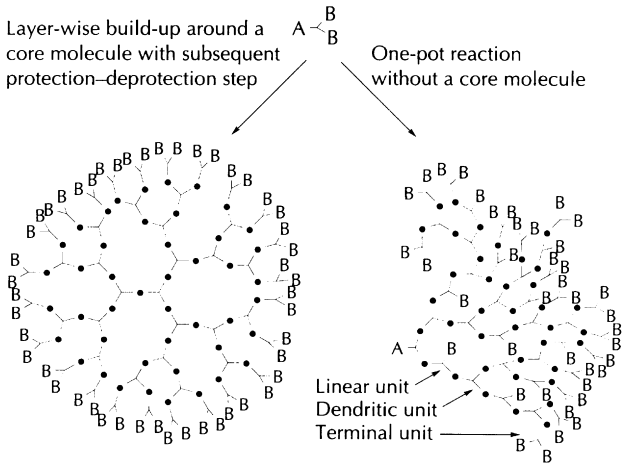

Fig. 2. Schematic descriptions of dendrimers (left) and hyperbranched polymers (right) built from AB2-monomers; (●) represents the bond formed between an A- and a B-group.

$$\frac{\partial^2 \beta \Delta\mu_2}{\partial \phi_2^2} = 2a^{(0)} + 4a^{(1)}(3\phi_2 - 2) + 3a^{(2)}(12\phi_2^2 - 12\phi_2 + 2) + 2A^{(1)} + (A^{(2)} + B^{(3)})(-14 + 48\phi_2 - 36\phi_2^2) + A^{(3)}(-38 + 384\phi_2 - 1188\phi_2^2 + 1440\phi_2^3 - 600\phi_2^4) + A^{(4)}2(-43 + 744\phi_2 - 4230\phi_2^2 + 115200\phi_2^3 - 16560\phi_2^4 + 12096\phi_2^5 - 3528\phi_2^6) + (B^{(1)} + B^{(2)})2(5 - 6\phi_2) + B^{(4)} \times 2(3 - 30\phi_2 + 66\phi_2^2 - 40\phi_2^3) + C^{(1)} \times 2(4\phi_2 - 3)(-15 + 54\phi_2 - 40\phi_2^2) + C^{(2)} \times 12(\phi_2 - 1)(3\phi_2 - 2) + C^{(3)}2(1 - \phi_2) \times (-19 + 161\phi_2 - 355\phi_2^2 + 225\phi_2^3) + C^{(4)} \times 4(11 - 20\phi_2)(\phi_2 - 1)^2 - \frac{1}{M\phi_2^2}. \quad (30)$$

4. Results and discussion

We first calculated the liquid–liquid coexistence curves for hyperbranched polyol/water systems using the LCT with no specific interaction correlation. Fig. 1 shows the cloud point curves of a hyperbranched polyol gen. 4/water system. This system exhibits a UCST behavior. The lines are predicted by the LCT. Open circles indicate experimental data. The calculated coexistence curves show that the critical point of the given system increases with the separator length (n). As shown in Fig. 2, the structure of a hyperbranched polymer is very different from that of a dendrimer. It is very difficult to define the separator length of the hyperbranched polymer, because it has the linear segment region in its structure. As shown in Fig. 1, the critical point varies with different values of the separator length (n). Taking into account the polydispersity of a separator length (n) for the hyperbranched polymer, one can correlate the experimental distribution data for n with a proper algebraic expression of a distribution function.

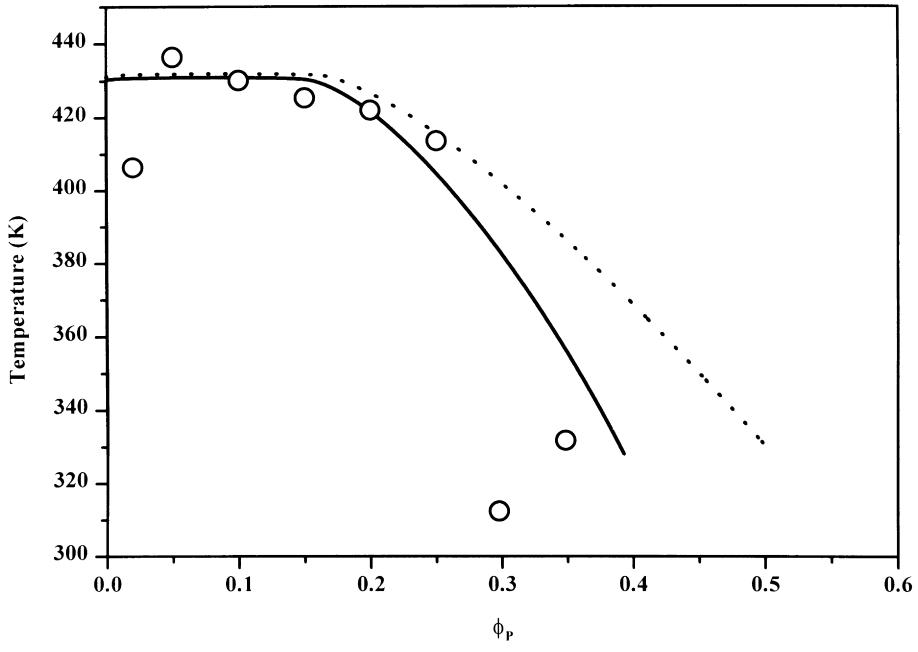

Fig. 3. Coexistence curves for the hyperbranched polyol gen. 4(M_w = 7.300)/water system. The solid line is predicted by the MLCT and the dotted line is calculated by the LCT. ○ indicate experimental data.

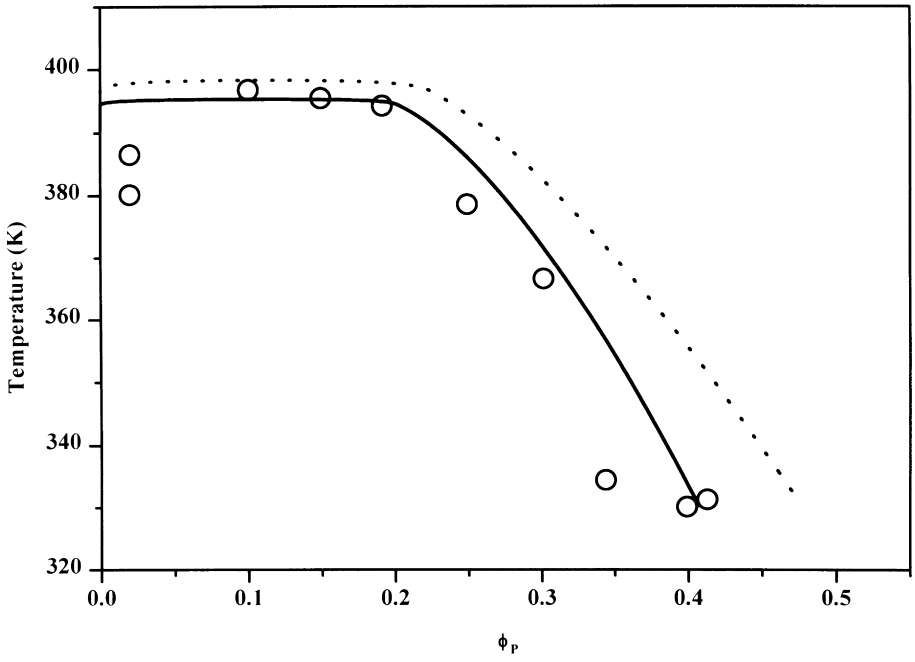

Fig. 4. Coexistence curves for the hyperbranched polyol gen. 3(M_w = 3.600)/water system. The solid line is predicted by the MLCT and the dotted line is calculated by the LCT. ○ indicate experimental data.

However, it is very difficult to obtain the experimental distribution curve for n. In this study, we set n as an adjustable model parameter so that our n values are mean separator lengths for the given systems.

Fig. 3 compares theoretical coexistence curves by the LCT (dotted line) with the modified lattice cluster theory (MLCT, solid line) that takes into account the specific interaction of strongly interacting components with experimental data for the system gen. 4(M_w = 7.300)/water. Open circles indicate experimental data. The MLCT shows better agreement with experimental data than that of the LCT. The model adjustable parameter values are n = 3.5, ε/k = 105.81 K and $\delta\varepsilon/k$ = 248.37 K.

Fig. 4 presents theoretical coexistence curves and experi-

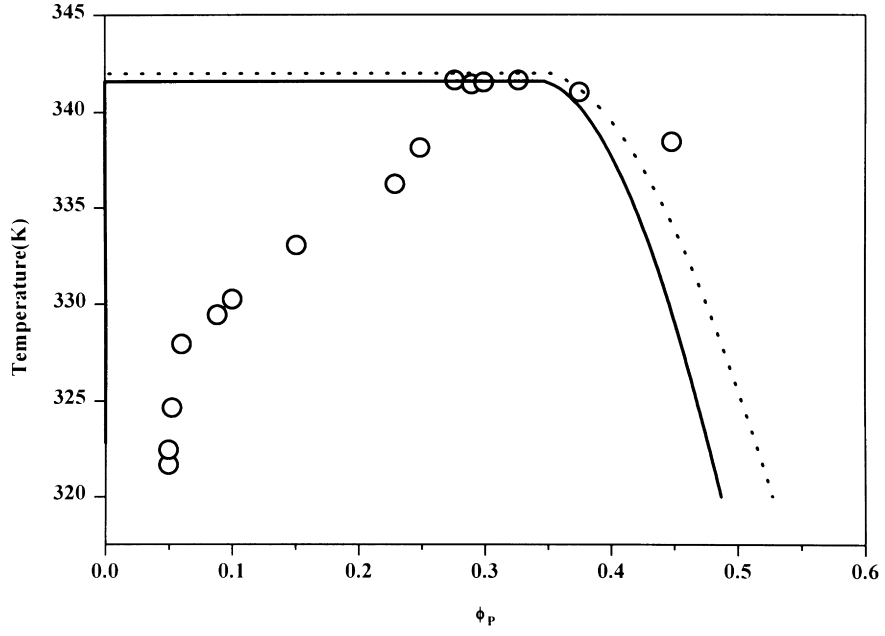

Fig. 5. Coexistence curves for the hyperbranched polyol gen. 2(M_w = 1.750)/water system. The solid line is predicted by the MLCT and the dotted line is calculated by the LCT. ○ indicate experimental data.

mental data for the system gen. 3 ($N_w = 3.600$)/water. Open circles indicate experimental data. The coexistence curves are predicted both by the LCT (dotted line) and the MLCT (solid line). The MLCT also describes the phase behavior of the system gen. 3/water better than that of the LCT. The model parameter values are $n = 6.0$, $\varepsilon/k = 94.57$ K and $\delta\varepsilon/k = 210.79$ K.

Fig. 5 shows coexistence curves for the system gen. 2/water. Open circles indicate experimental data. The solid line is calculated by this work and the dotted line is predicted by the LCT. The model parameter values are $n = 6.0$, $\varepsilon/k = 105.53$ K and $\delta\varepsilon/k = 223.21$ K. As shown in Fig. 5, there are large deviations between theoretical predictions and the experimental data in the dilute polymer concentration region.

According to Turner et al. [29], solubility of a hyperbranched polymer is largely dependent on the end-group structure. The solubility increases with the number of polar end groups of a hyperbranched polymer in a polar solvent. As both the LCT and the MLCT do not consider the contribution of the end-groups, it is difficult to predict the phase behavior of a hyperbranched polymer in the dilute polymer concentration region in which the end-groups of a polymer strongly interact with solvent.

5. Conclusion

The MLCT calculation shows a good agreement with experimental data. The model developed for the dendrimer can be appropriately applied to the hyperbranched polymer system. In this study, we introduced the contribution of the specific interaction to the free energy of mixing for the LCT. It, however, needs to take into account the end-group effect and the structure characteristic of the hyperbranched molecule.

Acknowledgements

This article was supported by the Non-directed Research Fund, Korea Research Foundation, 1996.

References

[1] Johansson M, et al. TRIP 1996;4:398.
[2] Tomalia DA, Dvornic PR. Nature 1994;372:617.
[3] Dagan R. C&EN 1996;3:30.
[4] Flory PJ. Principles of polymer chemistry. Ithaca: Cornell University, 1953.
[5] Huggins. J. Chem Phys 1941;9:440.
[6] Guggenheim EA. Mixtures. Oxford: Clarendon Press, 1952.
[7] Koningsveld R, Klientjens LA. Macromolecules 1971;4:637.
[8] Flory PJ. J Am Chem Soc 1965;87:1833.
[9] Flory PJ. Discuss Faraday Soc 1970;49:7.
[10] Patterson D, Delmas G. Trans Faraday Soc 1969;65:708.
[11] Sanchez IC, Lacombe RH. Macromolecules 1984;17:815.
[12] Backer JA, Fock W. Discuss Faraday Soc 1953;15:188.
[13] ten Brinke G, Karasz FE. Macromolecules 1984;17:815.
[14] Freed KF. J Phys A; Math Gen 1985;18:871.
[15] Bawendi MG, Freed KF, Mohanthy U. J Chem Phys 1988;87:5534.
[16] Bawendi MG, Freed KF, Mohanthy U. J Chem Phys 1988;88:2741.
[17] Nemirovski AM, Bawendi MG, Freed KF. J Chem Phys 1987;87:7272.
[18] Freed KF, Bawendi MG. J Phys Chem 1989;93:2194.
[19] Dudowicz J, Freed MS, Freed KF. Macromolecules 1991;24:5096.
[20] Freed KF, Dudowicz J. J Theor Chim Acta 1992;82:357.
[21] Dudowicz J, Freed KF. Macromolecules 1991;24:5076.
[22] Nemirovski AM, Dudowicz J, Freed KF. Phys Rev A 1992;45:7111.
[23] Panayiotou CG, Vera JH. Fluid Phase Equilib 1980;5:55.
[24] Renuncio JAR, Prausnitz JM. Macromolecules 1976;9:895.
[25] Panayiotou CG. Macromolecules 1987;20:861.
[26] Sanchez IC, Balazs AC. Macromolecules 1989;22:2325.
[27] Dudowicz J, Freed KF, Madden WG. Macromolecules 1990;23:4803.
[28] Lue L, Prausnitz JM. Macromolecules 1997;30:6650.
[29] Turner SR, Walter F, Voit BI, Mourey TH. Macromolecules 1994;27:1611.